Urban Forestry & Urban Greening 70 (2022) 127542

Contents lists available at ScienceDirect

Urban Forestry & Urban Greening

journal homepage: www.elsevier.com/locate/ufug

Traffic restrictions during COVID-19 lockdown improve air quality and reduce metal biodeposition in tree leaves

David Soba [a], Angie L. Gámez [a], José María Becerril [b], Raquel Esteban [b], Iker Aranjuelo [a,*]

[a] Instituto de Agrobiotecnología (IdAB), Consejo Superior de Investigaciones Científicas (CSIC)-Gobierno de Navarra, Avenida Pamplona 123, 31192 Mutilva, Spain
[b] Department of Plant Biology and Ecology, University of the Basque Country (UPV/EHU), c/Sarriena s/n, 48080 Bilbao, Spain

A R T I C L E I N F O

Keywords:
Biomonitoring
COVID-19
Lockdown
Metal deposition
Traffic emissions
Urban pollutants

A B S T R A C T

The coronavirus disease (COVID-19) has had a great global impact on human health, the life of people, and economies all over the world. However, in general, COVID-19ś effect on air quality has been positive due to the restrictions on social and economic activity. This study aimed to assess the impact on air quality and metal deposition of actions taken to reduce mobility in 2020 in two different urban locations. For this purpose, we analysed air pollution (NO_2, NO, NO_x, SO_2, CO, PM_{10}, O_3) and metal accumulation in leaves of *Tilia cordata* collected from April to September 2020 in two cities in northern Spain (Pamplona-PA and San Sebastián-SS). We compared their values with data from the previous year (2019) (in which there were no mobility restrictions) obtained under an identical experimental design. We found that metal accumulation was mostly lower during 2020 (compared with 2019), and lockdown caused significant reductions in urban air pollution. Nitrogen oxides decreased by 33%−44%, CO by 24%−38%, and PM_{10} by 16%−24%. The contents of traffic-related metals were significantly reduced in both studied cities. More specifically, significant decreases in metals related to tyre and brake wear (Zn, Fe, and Cu) and road dust resuspension (Al, Ti, Fe, Mn, and Ca) were observed. With these results, we conclude that the main reason for the improvement in urban air pollutants and metals was the reduction in the use of cars due to COVID-19 lockdown. In addition, we offer some evidence indicating the suitability of *T. cordata* leaves as a tool for biomonitoring metal accumulation. This information is relevant for future use by the scientific community and policy makers to implement measures to reduce traffic air pollution in urban areas and to improve environmental and human health.

1. Introduction

The increasing urbanization and concentration of human activities around cities has led to a worsening in urban air quality during recent decades (Grigoratos et al., 2014). Industrial activities are associated with gaseous pollutants and particulate matter emissions containing heavy metals, but urban transportation is also a significant contributor, and both negatively affect the lives and health of humans living in cities (World Health Organization, 2016). However, during the spring and summer of 2020 the lockdown measures imposed due to the outbreak of a novel coronavirus disease 2019 (COVID-19) offered a unique opportunity to assess the contribution of urban traffic to air pollution.

In December 2019, COVID-19 was described in Wuhan, China (Guan et al., 2020). From this date, COVID-19 has spread rapidly across the globe (World Health Organization, 2020), becoming a serious threat to all of humankind (Wang et al., 2020). After the first cases were confirmed in Spain at the end of January 2020, the numbers of cases and deaths increased quickly over the following weeks and months (NCE, 2020; Guirao, 2020), especially in the study area (Navarre and Basque Country) (Redondo-Bravo et al. 2020). Considering its highly contagious characteristics, COVID-19 has presented an extreme challenge to different countries, who have implemented different strategies depending on social, economic, and political factors (Han et al., 2020). Containment measures such as social distancing, quarantine, and isolation were among the most widely adopted to control the disease outbreak. The Government of Spain declared a state of emergency along with a lockdown on March 15th, 2020, including restricted social contact, the closing of restaurants, shops, and a large number of companies (Tobías et al., 2020; Briz-Redón et al., 2021). These measures were even stricter during the period March 30th to April 13th, when non-essential activities were prohibited. Because positive results were observed, on May 4th the lockdown restrictions were gradually relaxed until the

* Corresponding author.
E-mail address: iker.aranjuelo@csic.es (I. Aranjuelo).

https://doi.org/10.1016/j.ufug.2022.127542
Received 15 March 2021; Received in revised form 31 January 2022; Accepted 6 March 2022
Available online 12 March 2022

majority of the restrictions in most of the country were removed by June 21st with the end of the state of emergency. During the first wave of the COVID-19 pandemic and in response to its high severity, the Spanish lockdown was one of the strictest, along with China and Italy (Papandreou et al. 2020).

Due to the drastic reduction in economic and social activities, several studies have suggested that lockdown has dramatically improved air quality worldwide (Ambade et al., 2021; Bherwani et al., 2020; Gautam, 2020; Kumari and Toshniwal, 2020; Muhammad et al., 2020; Xu et al., 2020; Fan et al., 2021). In Spain specifically, nitrogen dioxide (NO_2), sulfur dioxide (SO_2), carbon monoxide (CO), ozone (O_3), and particulate matter (PM) with diameters ≤ 10 μm (PM_{10}) have varied significantly in a number of cities following the lockdown implemented during the COVID-19 outbreak (Martorell-Marugán et al., 2021; Tobías et al., 2020; Baldasano, 2020; Gautam, 2020). This temporal reduction in air pollutants, due mainly to urban traffic restriction, was a great opportunity to study and understand pollution sources and their impacts and consequences for air quality in cities worldwide, and this information could be employed by policymakers and authorities to develop effective and efficient future strategies to alleviate urban pollution levels.

However, most of these studies are based on satellite global data of air pollution caused by gaseous contaminants and particulate matter (PM) (Habibi et al., 2020), and studies at the local level monitored with ground-based stations in cities are still scarce and limited to gaseous contaminants and PM. This is a relevant issue, as ground-based data represents the pollution that people experience directly (Habibi et al., 2020) and this is severely affected by meteorological conditions (Baldasano, 2020). Besides, the majority of studies have been limited to or close to the most critical period of lockdown and did not continue after the restrictions were removed. Other urban contaminants like metals (Rai, 2016; Li et al., 2017; Soba et al., 2021) have not been given much attention in these studies. Recently, air pollutants (PM_{10}, NO_2, O_3) (Marquès et al., 2021) together with heavy metal exposure (Skalny et al., 2020) have been proposed as a relevant risk factor for COVID-19 and other respiratory infectious diseases, thus prompting the direct or indirect monitoring of these pollutants in populated areas during the COVID-19 outbreak. Only a few studies so far have examined these contaminants: (i) the study in Milan of Altuwayjiri et al. (2021) determining the presence of six redox-active metals with filters; and (ii) a study of the deposition of eight metals on a moss (*Pleurosium shreberi*) at several of sites in the industrial/urban metropolitan area of Moscow during June 2020 (Yushin et al., 2020).

Ground-based stations provide useful and almost real-time air quality information, but these are mainly for gaseous contaminants. Indeed, the use of these stations (in terms of numbers and spatial distribution) to monitor PM deposition and metals is restricted by their high cost (Aničić et al., 2011) and impact on the aesthetics of the urban environment. As a complement and/or alternative to these traditional chemical air pollution assessment methods, biomonitoring tools have recently gained interest specially using trees due to their unique characteristics. Foliar metal profiling is representative of atmospheric metal deposition (El-Khatib et al., 2020) and is proposed as an efficient biomonitoring method for urban pollution assessment with some advantages such as low cost, and if widely distributed, better recording of spatial air quality and appropriate for long time accumulation of pollutants (Smodiš et al., 2004; Tomašević et al., 2004; Doganlar et al., 2012, Martín et al., 2018). On the other hand, some limitations of biomonitoring are related to morphological structures, physiology and chemical composition of biological matrices can affect pollutant deposition (Jiang et al., 2018). Toxicity caused by pollutants and the non-ubiquitous presence of on plant species in urban gardens can limit its use for comparative studies of geographically diverse cities. Among urban trees, species of the native Eurasian genus *Tilia* are planted ubiquitously in city streets and parks, and previous studies by our group indicated an appropriate species to cope with air pollution in urban areas (Soba et al., 2021). Other studies (Piczak et al., 2003; Tomašević et al., 2004; Aničić et al., 2011; Serbula et al., 2013; Kalinovic et al., 2017) also use of these species to monitor heavy metal pollution in cities.

This study takes into account some of the limitations of other studies in assessing the temporary impact of COVID-19 restrictions at a local level from the lockdown to the end of summer on gaseous contaminants including ozone and PM, and on metal deposition. Additionally it explores the suitability of biomonitoring of trees in their role as essential and ubiquitous elements of any urban landscape. With this in mind, we hypothesized that due to the reductions in car use during COVID-19 lockdown, a decrease in air-borne heavy metals occurred and that this change could be measured by using urban tree leaves as biomonitoring tools. Therefore, to take advantage of the opportunity offered by this unprecedented situation and considering that Spain imposed and strict lockdown, and we conducted a previous study during 2019 in two cities with different edaphoclimatic conditions and traffic flow (San Sebastián and Pamplona), the main objective of the present work was to study urban air pollution changes by comparing data from the same periods in 2019 and 2020 in terms of metal accumulation in urban tree leaves in two locations. To our knowledge, no previous studies have reported the use of foliar metal profiling as an indicator of changes in air pollutants due to COVID-19 lockdown.

More specifically our objectives were to: (i) quantify potential improvement in air quality assessing gaseous levels of air pollutants during and after lockdown and during the preceding year; ii) quantify reductions in metal accumulation on *T. cordata* leaves due to traffic restriction; (iii) identify the source of traffic-related metals (pipeline emissions, tyre and brake wear, dust resuspension); (iv) determine the influence of meteorological conditions on urban air pollution during COVID-19 lockdown; (v) and assess the overall traffic impact on urban air quality.

2. Materials and methods

2.1. Study area

The study was conducted in two different cities in northern Spain in the Autonomous Communities of Navarre (Pamplona, herein PA; 42º48'46''N 1º38'48''W) and the Basque Country (San Sebastián, herein SS; 43º19'09''N 1º58'44''W) (Fig. S1). The populations of the two cities were: PA (201,653 people) and SS (187,415 people) (Instituto Nacional de Estadística, 2019). The two cities were chosen for their similar population and because they have very different traffic flow, climatic and socio-economic characteristics. On the one hand, PA is an interior continental city in the transition between Atlantic and Mediterranean climates and, on the other hand, SS is a coastal and very touristic city with a temperate Atlantic climate and a precipitation regime double that of PA. In both cities, two high traffic-density streets were chosen for foliar sampling: Avenida del Ejército (PA) and Paseo del Árbol de Gernika (SS).

2.2. Air pollution, traffic density, and meteorological data

For air pollution concentrations and weather variables, this study compiled data daily from monitoring stations in PA (Gobierno de Navarra) and SS (Gobierno Vasco, 2020). The air pollution data included daily atmospheric concentration levels of NO_2, NO, NO_x, SO_2, CO, PM_{10}, and in the case of PA, also O_3. Daily levels of CO (in mg/m^3), NO_2 (in μg/m^3), NO (in μg/m^3), NO_x (in μg/m^3), PM_{10} (in μg/m^3), O_3 (in μg/m^3), and SO_2 (in μg/m^3) for each station and day from March 1st-September 30th, 2019 and March 1st-September 30th 2020 were collected from the online portal of the Navarre Government (https://gobiernoabierto.navarra.es/es/open-data/datos/calidad-del-aire-navarra) and from the online portal of the Basque Country in SS (https://opendata.euskadi.eus/catalogo/-/calidad-aire-en-euskadi/).

Taking into account the different lockdown phases of the COVID-19 outbreak in Spain (see Introduction section), the pollutant levels were analysed as three periods in 2019 and 2020: strict lockdown (March 15th to May 3rd, 50 days), relaxed lockdown (May 4th to June 21th, 49 days) and normality (after lockdown; June 22th to September 30th, 100 days).

Traffic density data were obtained from the City Council of Pamplona and San Sebastián. In both cases, the point of measurement was in the same street and near to the selected sampling point.

Daily meteorological data were downloaded for the same periods from the online portal of the Navarre Goverment in PA (http://meteo.navarra.es/estaciones/estacion.cfm?IDestacion=455) and from the online portal of the Basque Country in SS (https://opendata.euskadi.eus/./-/estaciones-meteorologicas-lecturas-recogidas-en-2019/). The meteorological stations closest to the cities were chosen to obtain the meteorological variables of interest: average, maximum, and minimum temperature (°C), precipitation (mm), wind speed (km/hr), irradiation (W/m^2), and atmospheric pressure (hPa).

2.3. Sampling

In the two locations, leaves were sampled from deciduous small-leaved lime (*T. cordata*) during the sampling period of April-October in 2019 and 2020. In each city, a street with high traffic density was chosen for foliar sampling (Avenida del Ejército in PA and Paseo del Árbol de Gernika in SS). Collection of the samples was carried out according to the standardized protocol exactly as described in Soba et al. (2021). In brief, for each location six replicates were taken for each sampling time, each comprising five healthy fully developed leaves randomly detached from a height of 2.0–2.5 m above the ground while wearing polyethylene gloves to avoid contaminating the samples, which were then rapidly transported to the laboratory. Once in the laboratory, samples were dried at 65ºC for 48 h and stored under a low-humidity atmosphere until grinding and further analysis to estimate absorbed and deposited pollutants.

2.4. Element analyses

With the aim of a comprehensive view of leaf anthropogenic contamination, the presence and concentrations of a range of elements (i.e., Al, B, Ca, Cr, Cu, Fe, K, Mg, Mn, Na, Pb, P, Rb, Si, S, Sr, Ti, Tl, and Zn) were analysed in leaf samples that previously had been ground to a fine powder. For the mineral concentration analysis, 20 mg of material and 5 ml of nitric acid-hydrogen peroxide (33%) (4:1) were digested in a microwave digestion system for 20 min at 220ºC. After digestion, samples were diluted with 20 ml of ultrapure water. The analysis was carried out at the ionomic service of the Centre for Edaphology and Applied Biology (Murcia, Spain) using ICP/OES (inductively coupled plasma/optical emission spectrometry, iCAP 6500 Duo, Thermo Fisher Scientific, Waltham, USA). Calibration curves were generated using standard stock solutions at different concentrations. The detection limit for all metals was established at 0.01 mg kg^{-1}.

2.5. Statistical analysis

Statistical analyses were performed with IBM SPSS Statistics for Windows, Version 20.0. (IBM Corp. Armonk, NY, USA). Statistical differences between measurements of the different locations and years were evaluated with analyses of variance (ANOVA). All data were tested for normality (Kolmogorov-Smirnof test) and homogeneity of variances (Levene's test). Tukey post hoc tests were used to determine statistical differences between locations. To study correlations between the variables, Pearson correlation analyses were calculated. For ANOVA and Pearson correlation analysis, the results were considered to be significant when $p < 0.05$. Principal component analysis (PCA) for the two cities and years was conducted using STATGRAPHICS Centurion XV (StatPoint, Inc., Warrenton, VA, USA) software.

3. Results and discussion

3.1. Traffic density across the cities and lockdown and meteorological effects on pollutant levels

Assessment of the average traffic flow in a regular year (2019) indicated that San Sebastián (SS) had almost double the traffic of Pamplona (PA), with 11,000 and 6,500 vehicles/day respectively (Fig. 1). During the strict lockdown (March 15th to May 3rd; Fig. 1) the traffic flow greatly decreased 82% in SS and 77% in PA. At this point, the difference in traffic flow between the two cities was at its lowest, with only 485 vehicles/day difference between them (traffic flow remained higher in SS). During the relaxed lockdown (May 4th to June 21th) the traffic flow increased progressively, but the number of vehicles/day and the slope was always higher in SS. Finally, during the third phase (May-October) the traffic flow recovered to values similar to those of the previous year (2019). Interestingly, the expected reduction in traffic flow was very different between the cities since it was negligible in PA but SS showed a great reduction due to the low mobility observed to tourist locations.

Data provided by ground-based monitoring stations allowed us to assess the impact of the lockdown measures on gaseous contaminants and PM in two northern Spanish cities. In general, higher pollutant concentrations (NO_x, CO, and PM_{10}) were found in SS during both years and all phases (Table S1) when compared to PA, which is in accordance with the observed higher traffic rates (Fig. 1). We analysed the percentage variations in pollutant levels between 2019 and 2020 and their statistical significance for each city and each of the lockdown phases. The results are shown in Table 1. This exploratory analysis showed significant variations in pollutant levels across different types of lockdown in Spain. As expected, and in accordance with previous local studies in Spain (Sicard et al., 2020; Tobías et al., 2020; Martorell-Marugán et al., 2021; Briz-Redón et al., 2021), levels of NO_2, NO, and NO_x during the lockdown in both cities were temporarily and substantially reduced with the variation ranging from − 41 to − 45% for PA and − 33 to − 41% for SS (Table 1). Compared with the previous year, levels of O_3 were reduced only during the strict lockdown, and these reductions were only significant in SS (−17%). Reductions in these pollutants were expected due to their close correlation with traffic emissions (Choi et al., 2009; Tobías et al., 2020); nevertheless, considering that the numbers of vehicles during the strict lockdown were quite similar in the two cities (Fig. 1), a more drastic reduction in traffic flow occurred in SS and consequently greater reductions in pollutants in SS should be expected. We observed greater differences in SS for other air pollutants associated with traffic such as CO with − 24% in PA and − 38% in SS, and for PM_{10}, which is a parameter closely related to heavy

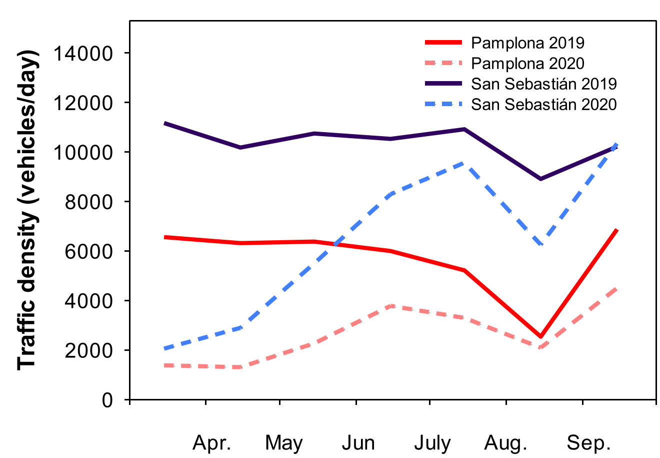

Fig. 1. Traffic density (vehicles/day) in the sampling points in Pamplona and San Sebastián during the leaf collecting periods in 2019 and 2020.

Table 1
Percentage of variation in daily atmospheric concentration levels of NO_2, NO, NO_x, PM_{10}, CO, SO_2, and O_3 between 2019 (normality) and 2020 (COVID-19 lockdown) at two sites (Pamplona and San Sebastián) for three periods of time: strict lockdown (March 15th to May 3rd, n = 50 measures); relaxed lockdown (May 4th to June 21th, n = 49 measures) and Normality (June 22th to September 30th, n = 100 measures). The coefficients in bold showed significant differences between years for the same period.

Location	Pamplona			San Sebastián		
Periods/Atmospheric levels	Strict lockdown	Relaxed lockdown	Normality	Strict lockdown	Relaxed lockdown	Normality
NO_2	**-45.41****	**-37.02****	**-26.52****	**-33.14****	-10.83	3.16
NO	**-41.98***	**-43.58****	**-37.29****	**-41.07****	-17.84	-13.98
NO_X	**-44.25****	**-38.71****	**-29.42****	**-36.02****	-13.67	-4.84
PM_{10}	-8.39	13.77	**-16.44***	**-24.20****	3.32	**-22.52****
SO_2	4.22	-11.57	3.02	**13.36***	5.96	6.36
CO	**-24.56****	**-25.69****	-3.37	**-38.25****	**14.66***	6.83
O_3	-8.50	8.05	**8.29***	**-16.64****	6.41	-0.04

Asterisks indicate significant differences: * $p < 0.05$, **$p < 0.01$.

metal pollution (Sternbeck et al., 2002; Lough et al., 2005; Hu et al., 2012) (Table 1). In any case, these reductions were lower than reductions observed in other more populated cities in Spain such as Madrid and Barcelona (Baldasano, 2020; Briz-Redón et al., 2021).

During the relaxed lockdown phase (2nd phase) and after lockdown (3rd phase), the benefits of reductions in air pollution were only significantly in PA, which was likely due to the faster recovery rates in SS traffic flow (Fig. 1). Nonetheless, during the 3rd phase a significant decrease in PM_{10} was observed in both cities (Table1). Contrary to the other pollutants in PA, the levels of ground-level ozone increased during the 3rd phase, whereas in SS the levels decreased during the strict lockdown but remained similar to 2019 values during the 2nd and 3rd phases. Significant increases in ozone levels across the globe during 2020 were also observed (Habibi et al., 2020, Sicard et al., 2020) and this effect could be related to decreased ozone titration due to a sustained decline in NO production (Huang et al., 2018). Indeed, the sustained decline in NO_x in PA during the three studied phases, in contrast to SS, could help to explain the observed differences. Similarly, in a multi-city study carried out during the Spain lockdown, Briz-Redón et al. (2021) only showed significant increases in O_3 in two of the 11 studied cities. Such results have major implications for public health, mainly in respiratory illnesses, and the vulnerability to COVID-19 deserves much more attention if traffic management regulation in cities is modified. In fact short- and long-term exposure to O_3 is associated with cardiovascular and respiratory mortality (Doherty et al., 2017). Also, it is known that chronic or short-term exposure to O_3, NO_x and PM_{10}, as possible carriers of viruses or bacteria has a significant negative impact on the human immune system and the pathogenesis of severe respiratory infections (Zoran et al., 2020).

Although these pollutants are related to traffic emissions, other natural and anthropogenic sources (industrial sources, shipping and dockyard emissions, construction works, dust re-suspension) should not be discarded (Martorell-Marugán et al., 2021). Consequently, attributing specifically or quantifying the effect of lockdowns to changes in air pollutants are not always possible because other factors might have influenced the observed changes, such as meteorological conditions (Baldasano, 2020) and/or long-distance transport of air pollutants. For instance, both locations were also selected for their contrasting climatic characteristics. While PA is located in the transition between the Mediterranean and Atlantic climate zones, SS has a typical Atlantic climate. Therefore, to better understand the influence of several meteorological parameters on air pollutants a correlation analysis was performed between these multiple variables during the study periods of 2019 and 2020 (Table 2). While highly positive correlations were found in 2019 between daily temperatures (average, maximum and minimum) and daily NO_x, CO and PM_{10} concentrations, their correlation was not significant and it was even negative in 2020. Air temperature has been previously positively correlated with the concentration of CO and NO_x (Ghahremanloo et al., 2021), O_3 (Varotsos et al., 2019) and PM_{10} (Radzka, 2020). However, in 2020, the temperature in both cities was higher than in 2019, indicating that other environmental factors may have been responsible for the decrease in air pollutants levels during 2020. The trend in the rest of the meteorological covariates did not align with changes in the studied air pollutants. Therefore, we can conclude that meteorological factors were not responsible for the significant reductions in NOx, CO and PM_{10} levels in the atmosphere during the spring and summer of 2020, and that the extent of the reductions in these two cities is consistent with the severity of the lockdown and the associated dramatic reduction in social and economic activities, which in turn were mainly related to the great decrease in urban traffic (Fig. 1). Finally, the slight increase in O_3 (8%; $P = 0.045$) observed in PA after lockdown (Table 1), could not be explained by meteorological factor, NO_x levels or traffic flux and, therefore, another factor (or combination of factor) could be behind this specific increase.

3.2. *Effect of lockdown on foliar metal profiling*

Most studies carried out so far to assess the lockdown effect on air

Table 2
Pearson correlation coefficients between air pollutants (NO_2, NO, NO_x,PM_{10}, CO, SO_2, and O_3) and meteorological variants (average temperature (Ave. Tª), maximum temperature (Max. Tª), minimum temperature (Min. Tª), precipitation (Precip.), radiation (Radiat), wind velocity (Wind), and pressure (Pressure). Data from Pamplona and San Sebastián between March 15th and September 30th are shown. Correlations for 2019 and 2020 are presented separately. The coefficients shown in bold are significant. n = 199 measures.

	Ave. Tª		**Max. Tª**		**Min. Tª**		**Precip.**		**Radiat.**		**Wind**		**Pressure**	
	2019	2020	2019	2020	2019	2020	2019	2020	2019	2020	2019	2020	2019	2020
NO_2	**,368****	**-,212****	**,404****	**-,271****	**,265****	**-,161***	-.010	-.105	.159	-.266	-.152	.131	.227	.212
NO	**,402****	-.008	**,372****	-.067	**,342****	.013	**,258****	-.096	.192	-.038	-.019	.053	.203	**,375****
NO_x	**,405****	-.121	**,408****	**-,185***	**,320****	-.083	.131	-.108	.185	-.190	-.089	.103	.228	**,304***
PM_{10}	**,570****	-.131	**,488****	-.102	**,495****	-.154	-.055	**-,245****	**,360***	**,342***	**,164***	.154	**,283***	.148
SO_2	-.056	**,219****	**,191***	**,253****	**-,172***	.112	.057	-.017	.250	.189	**-,285****	**-,174***	.114	-.070
CO	**,651****	-.047	**,401****	-.118	**,642****	.010	-.034	-.059	**,376****	.061	**,292****	**,279****	**,447****	-.082
O_3	-.071	-.129	**-,389****	-.209	**,361****	-.061	**-,303***	-.268	.021	.167	**,501****	**,755****	.011	-.264

Asterisks indicate significant differences: * $p < 0.05$, **$p < 0.01$.

quality were performed on gaseous pollutants and there is a lack of studies on other urban pollutants, such as metals, that severely affect human health. To this end, we assessed changes in urban pollution due to COVID-19 lockdown and the concentrations of 18 elements were analysed (Al, B, Ca, Cr, Cu, Fe, K, Mg, Mn, Na, Pb, P, Rb, Si, S, Sr, Ti, Tl, and Zn). Furthermore, we carry out this study by analysing metal accumulation in *T. cordata* leaves to test the suitability of *T. cordata* as a valid methodology to biomonitor urban metal pollution. The multielement analyses were performed by ICP/OES spectrometry. The mean concentrations of metals as determined by ICP/OES of *T. cordata* leaves from two different cities in Spain and during the 2019 and 2020 growing seasons are shown in Table 3. The foliar concentrations of the different analysed metals were in accordance with the average values reported in the literature for *Tilia* spp. (Tomašević et al., 2004, Aničić et al., 2011; Aničić et al., 2011; Sawidis et al., 2011; Kalinovic et al., 2017; Soba et al., 2021). Even though both cities are similar in population, the concentrations of the majority of elements (Al, Cr, Cu, Fe, Pb, Rb, Ti and Zn) were higher in SS than PA, and only Mn and Sr were in higher concentration in PA (Table 3 and Fig. 2). These observations are in accordance with the higher atmospheric pollutant contents measured by monitoring stations in this city (Table 2) and the higher traffic density of SS (Fig. 1) when compared to PA. Similar to the results for the gaseous contaminants (Table 1), the percentage of reduction in the elements was higher in PA (27%) than in SS (19%) (Table 3) and this seems to indicate that both types of pollutants come from traffic-related sources. Likewise, the percentage of variation between years was also calculated for each location. The biggest difference between years was observed for five metals whose contents significantly reduced during 2020 in both cities: Al, Cu, Fe, Mn and Zn. Additionally, Sr in PA and Pb and Ti in SS also showed reduced concentrations in 2020 ($p < 0.05$). As reported previously (Wåhlin et al., 2006; Bretzel and Calderisi, 2006; Adamiec et al., 2016; Martín et al., 2018; Soba et al., 2021), all of these heavy metals have traffic-related origins. The accumulation trends for these metals in both cities for the period March to October 2019 and 2020 are shown in Fig. 2. A progressive accumulation of metals during the growth and development of leaves was observed, and corresponded to the accumulation of particles on the leaf surface, but metal accumulation was mostly lower along the studied period during 2020.

Urban emissions of heavy metals related to traffic can be defined by three different sources: (a) vehicle exhaust emissions, (b) vehicle non-exhaust emissions (i.e., tyre abrasion and brake wear), and (c) dust resuspension from the roadway (Lough et al., 2005; Wang et al., 2021). Vehicle exhaust emissions are associated with Zn, Pb, Ni, and Cr (Johansson et al., 2009; Men et al., 2018). Metals like Zn, Cu and Pb have been associated with dust from tyre abrasion (Schauer et al., 2006; Hjortenkrans et al., 2007; Adamiec et al., 2016) with Zn being the most abundant heavy metal from tyre wear (Adamiec et al., 2016). In addition, Fe, Zn and Cu (Adachi and Tainosho, 2004; Johansson et al., 2009; Grigoratos and Martini, 2015), but also other metals such as Al, Ca, Mn, Ti, and Pb have been reported to originate from brake wear (Adachi and Tainosho, 2004; Hjortenkrans et al., 2007; Kukutschová et al., 2011). Finally, Al, Ca, Fe, Mg, Mn, and Ti are all typical geological marker elements, suggesting that resuspension controls their aerosol abundance (Sternbeck et al., 2002; Wang et al., 2021).

To reduce the complexity of the multivariate data and identify patterns, principal component analysis (PCA) was performed (Fig. 3). The PCA revealed that the first two principal components explained 61.3% of total variation between years and locations. The loading plot revealed that the metals Al, Zn, Cu and Fe, strongly correlated with both tyre and brake wear from traffic origins, are grouped and explained part of the variation observed in PC1 (38,31%) (Fig. 3). Furthermore, correlation analysis showed that Zn had the highest correlation with Cu and Fe during 2019 ($r > 0.5$; $p < 0.01$); however, the same correlations were slightly lower or not significant (Fe-Zn) during 2020. This indicates a common origin (in this case from brakes and tyres) and a reduction in the source during 2020 (probably from reduced traffic due to the lockdown (Fig. 1)) as indicated by the reduction in the three metals in both cities during 2020 and the lower correlation when compared with the previous year. On the other hand, PC2 (22.97% of the total variance) was in part determined by content of Sr, Mn, B, Mg and Fe. A remarkable decrease of Fe, Sr, Mn and Mg was observed mainly in Pamplona during pandemic lockdown.

By using PCA, the traffic-related origin of these metals was validated. PCAs were conducted separately for the two growing seasons to illustrate the relationships between the analysed elements (Tables 4, 5). In our analysis we found stronger correlations between elements during the 2019 growing season 2020 (Tables 4 and 5). Metals related to traffic pollution (Al, Cr, Cu, Fe, Mn, Pb, Ti, Zn) were always significantly correlated during 2019 (only Mn-Pb and Mn-Ti were not significant). On the other hand, during 2020 the correlation was lower or not significant between these traffic-related elements. All this suggests that the main source of urban pollution, in this case traffic emissions, were greatly

Table 3
Average values and percentage of variation in foliar elements (Al, B, Ca, Cr, Cu, Fe, K, Mg, Mn, Na, Pb, P, Rb, Si, S, Sr, Ti, Tl and Zn) between 2019 and 2020 in Pamplona and San Sebastián, Spain. Data correspond to the mean of five replicates±SE. The coefficients in bold show significant differences for the elements between years in each city.

Location	Pamplona			San Sebastián		
Year	2019	2020	Dif.	2019	2020	Dif.
Al (mg/Kg)	94.1 ± 6.21	75.2 ± 6.00	**-20.14****	184.5 ± 15.28	141.3 ± 6.36	**-23.38****
B (mg/Kg)	68.16 ± 10.95	64.84 ± 3.44	-4.86	63.78 ± 4.00	62.43 ± 4.11	-2.11
Ca (g/100 g)	1.94 ± 0.13	1.43 ± 0.08	**-26.05****	2.31 ± 0.12	2.01 ± 0.08	**-12.94***
Cr (mg/Kg)	1.78 ± 0.18	1.98 ± 0.25	11.27	2.11 ± 0.27	2.56 ± 0.48	21.33
Cu (mg/Kg)	8.98 ± 0.36	7.48 ± 0.38	**-16.66****	9.50 ± 0.28	8.70 ± 0.32	**-8.42***
Fe (mg/Kg)	277.8 ± 18.68	149.5 ± 8.18	**-46.19****	282.9 ± 25.32	222.6 ± 9.88	**-21.3***
K (g/100 g)	0.97 ± 0.04	1.14 ± 0.04	**18.27****	0.75 ± 0.08	0.68 ± 0.03	-10.06
Mg (g/100 g)	0.47 ± 0.02	0.25 ± 0.01	**-48.03****	0.30 ± 0.01	0.33 ± 0.01	7.74
Mn (mg/Kg)	70.5 ± 3.25	59.05 ± 2.22	**-16.24****	53.92 ± 2.06	40.94 ± 2.14	**-25.46****
Na (g/100 g)	0.02 ± 0.00	0.03 ± 0.00	**30.27****	0.16 ± 0.02	0.11 ± 0.01	**-29.03****
Pb (mg/Kg)	1.01 ± 0.10	1.09 ± 0.10	6.80	1.78 ± 0.19	1.38 ± 0.09	**-22.55****
P (g/100 g)	0.14 ± 0.01	0.17 ± 0.01	17.90	0.14 ± 0.00	0.14 ± 0.00	2.33
Rb (mg/Kg)	4.57 ± 0.32	5.53 ± 0.27	**20.78***	6.17 ± 0.44	5.61 ± 0.34	-9.05
Si (g/100 g)	0.07 ± 0.00	0.08 ± 0.01	12.49	0.11 ± 0.01	0.15 ± 0.01	**45.39****
S (g/100 g)	0.30 ± 0.01	0.23 ± 0.01	**-21.75****	0.16 ± 0.00	0.17 ± 0.00	1.54
Sr (mg/Kg)	267.6 ± 23.98	138.3 ± 7.03	**-48.30****	112.8 ± 7.16	108.1 ± 5.15	-4.13
Ti (mg/Kg)	6.27 ± 0.66	5.01 ± 0.70	-20.09	11.75 ± 0.96	9.63 ± 0.45	**-18.04****
Tl (mg/Kg)	12.12 ± 0.63	13.98 ± 1.35	15.35	10.68 ± 1.02	11.61 ± 1.28	8.74
Zn (mg/Kg)	28.11 ± 1.41	24.19 ± 1.11	**-13.95****	31.03 ± 1.42	24.82 ± 0.69	**-20.03****

Asterisks indicate significant differences: * $p < 0.05$, ** $p < 0.01$.

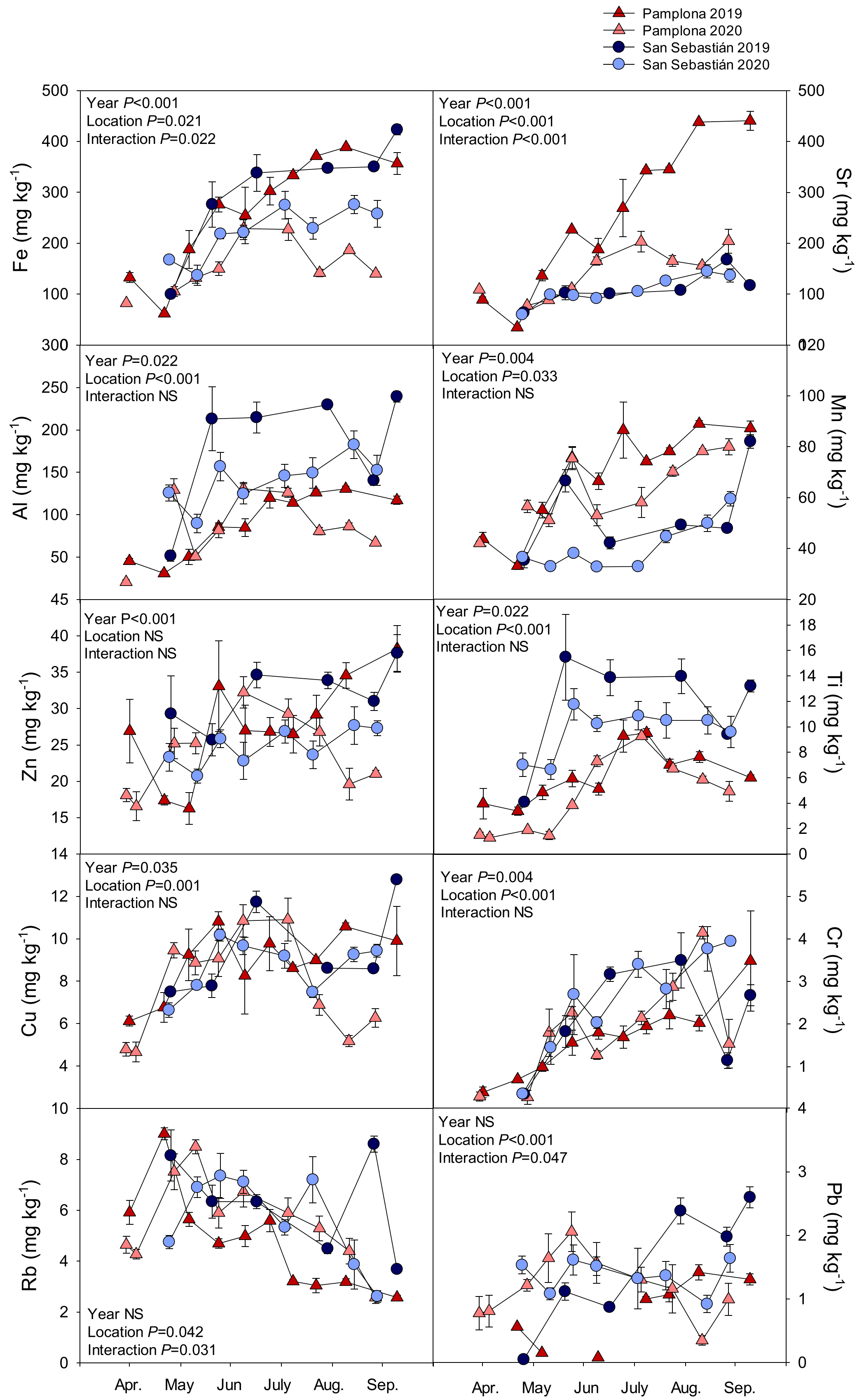

Fig. 2. Differential effects of location (Pamplona and San Sebastián) and year (2019 and 2020) on heavy metals related to traffic and/or industrial emissions. Data correspond to the mean of five replicates±SE. Results of two-way ANOVA are shown in the upper part of each panel ($P < 0.05$). NS, not significant.

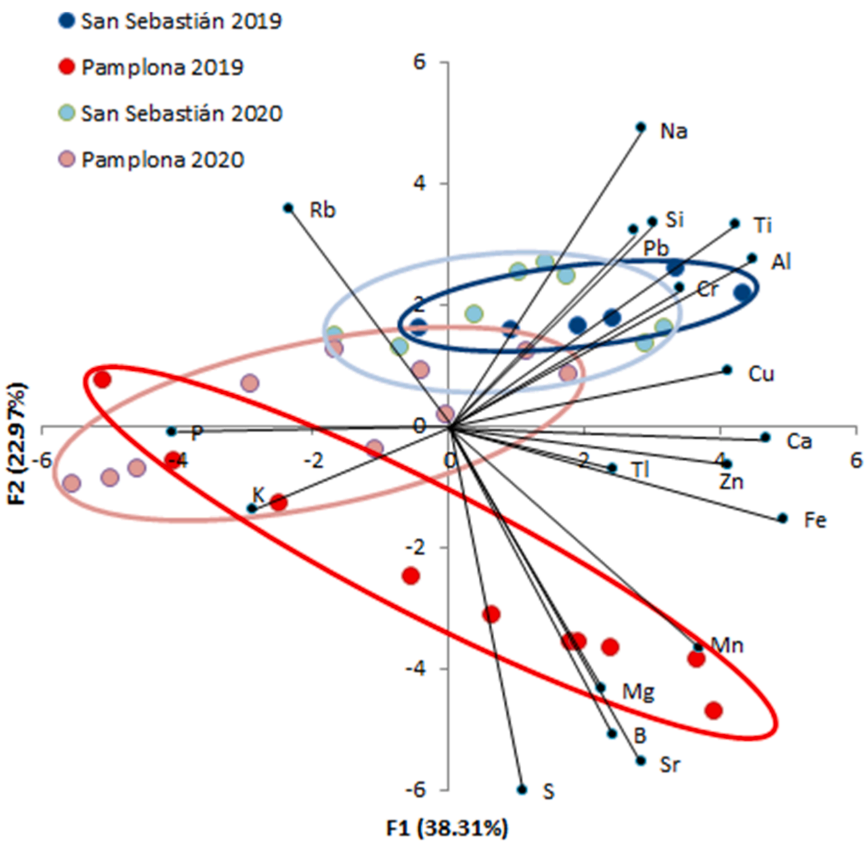

Fig. 3. Graphic representation of principal component analysis (PCA) and scatter plot distribution of the different elements in Pamplona and San Sebastián during the leaf collecting periods in 2019 and 2020 (April-September). Five replicates were examined per location and sampling point.

Table 4
Pearson correlation coefficients between elements (Al, B, Ca, Cr, Cu, Fe, K, Mg, Mn, Na, Ni, Pb, P, Rb, Si, S, Sr, Ti, Tl and Zn) measured by ICP/OES in leaves of *T. cordata* during the 2019 vegetative season in Pamplona and San Sebastián. The shade of red/blue indicates the strength of the negative/positive correlation, respectively; dark red/blue to light red/blue indicates stronger to weaker correlations.

	Al	B	Ca	Cr	Cu	Fe	K	Mg	Mn	Na	Pb	P	Rb	Si	S	Sr	Ti	Tl
B	.065																	
Ca	,594**	,354**																
Cr	,757**	.211	,439**															
Cu	,502**	.228	,434**	,515**														
Fe	,725**	,589**	,701**	,759**	,661**													
K	-,586**	-.112	-,338**	-,514**	-,258*	-,580**												
Mg	-.125	,842**	,307*	.039	.203	,423**	.070											
Mn	,317*	,818**	,634**	,355**	,399**	,761**	-,440**	,794**										
Na	,790**	-,389**	.231	,540**	.181	,252*	-,475**	-,523**	-.175									
Pb	,680**	-.224	,592**	,418**	,437**	,463**	-.289	-,434**	-.107	,587**								
P	-,455**	-,581**	-,589**	-,526**	-,324*	-,658**	,512**	-,464**	-,677**	-.152	-.009							
Rb	-,276*	-,675**	-,533**	-,400**	-,297*	-,744**	,591**	-,511**	-,768**	.133	-.089	,598**						
Si	,732**	.136	,466**	,499**	,446**	,482**	-.143	-.030	.219	,533**	,486**	-,367**	.016					
S	-.092	,776**	,484**	.014	.104	,467**	-.031	,756**	,740**	-,526**	-.180	-,374**	-,695**	-.076				
Sr	.032	,797**	,666**	.103	.225	,587**	-.147	,812**	,853**	-,430**	-.124	-,557**	-,749**	.014	,919**			
Ti	,932**	-.019	,416**	,652**	,403**	,574**	-,480**	-.195	.196	,786**	,548**	-,333**	-.093	,777**	-.193	-.108		
Tl	,338**	,422**	,306*	.209	.225	,497**	-,418**	,430**	,722**	.010	-.121	-,402**	-,466**	.112	,337**	,366**	,280*	
Zn	,459**	.135	,478**	,413**	,503**	,552**	-,512**	.072	,424**	,296*	,421**	-,269*	-,374**	.208	.143	,264*	,344**	.201

Asterisks indicate significant differences: * p<0.05, ** p<0.01

Asterisks indicate significant differences: * $p < 0.05$, ** $p < 0.01$.

Table 5
Pearson correlation coefficients between elements (Al, B, Ca, Cr, Cu, Fe, K, Mg, Mn, Na, Ni, Pb, P, Rb, Si, S, Sr, Ti, Tl and Zn) measured by ICP/OES in leaves of *T. cordata* during the 2020 vegetative season in Pamplona and San Sebastián. The shade of red/blue indicates the strength of the negative/positive correlation, respectively; dark red/blue to light red/blue indicates stronger to weaker correlations.

	Al	B	Ca	Cr	Cu	Fe	K	Mg	Mn	Na	Pb	P	Rb	Si	S	Sr	Ti	Tl
B	-.004																	
Ca	,427**	-.037																
Cr	,574**	-.107	,474**															
Cu	,570**	.092	,318**	,275*														
Fe	,856**	-.107	,319**	,543**	,651**													
K	-,363**	-.190	-,347**	-.190	-.115	-.064												
Mg	,523**	.141	,534**	,395**	,440**	,386**	-,458**											
Mn	-.099	-.060	,302**	,345**	-.183	-.027	.196	-.130										
Na	,470**	.030	,515**	,502**	,369**	,315**	-,565**	,621**	-.167									
Pb	.201	-.090	.108	.068	,314*	.158	-.108	.200	-.199	,357**								
P	.085	.187	-.135	-.077	.097	.178	,287*	-.061	.047	.023	.098							
Rb	-.120	.194	-,488**	-,276*	,240*	-.033	,232*	.081	-,406**	-.150	.073	.122						
Si	,409**	,568**	,313**	.219	,260*	,236*	-,428**	,560**	-.104	,236*	.010	-,227*	.137					
S	-,336**	-.214	-.049	-.001	.127	-.171	,517**	-,333**	,367**	-,345**	-.015	-.112	-.010	-,292*				
Sr	-.083	-.116	,506**	.190	-.106	-.022	.210	-.053	,539**	-,281*	-.153	-,388**	-,449**	.102	,451**			
Ti	,766**	-.027	.167	.224	,602**	,744**	-.132	,319**	-.098	.171	.247	.069	.032	,323**	-.039	.027		
Tl	-.176	-.235	-.187	.170	-,328*	-.130	,258*	-,319*	,788**	-,363**	-.189	-.179	-,309*	-.195	,335*	,372**	.029	
Zn	.082	-.142	.095	.046	,418**	.117	.105	.168	.195	-.014	.115	-.082	.088	-.140	,422**	.141	,398**	,298*

Asterisks indicate significant differences: * p<0.05, **p<0.01

Asterisks indicate significant differences: * $p < 0.05$, ** $p < 0.01$.

reduced during 2020.

Al, Fe and Ti deserve special attention because their correlations were always highly positive in both years ($p < 0.01$; Tables 4–5), again indicating a common origin for the metals. Likewise, when we looked at decreases in metal contents in both locations between 2019 and 2020, the same three elements were observed (although the decrease in Ti was not significant in PA) (Table 1). Elements such as Si, Ca, Mn, Al, Fe and Ti have been proven to have a crustal origin (Sternbeck et al., 2002; Wang et al., 2021) and therefore this decrease in Al, Fe and Ti can be attributed mainly to a decrease in the tyre-shear resuspension of crustal materials due to the lower traffic intensity during the lockdown. Also, the multiple strong correlations ($r > 0.7$; $p < 0.01$) observed between Ca/Fe, Si/Al and Si/Ti reinforce this theory. The observed significant decrease in Mn content in both cities during 2020 may have the same crustal origin as suggested in previous works (Sternbeck et al., 2002; Wang et al., 2021); however, the low correlation between this metal and Al, Ti and Si during 2019 make us cautious about their common origins.

Calcium is a component of detergent additives included in common engine oil (Cadle et al., 1997). The reduction in Ca in both locations during 2020 and the positive correlations with traffic-related metals such as Ca/Al, Ca/Fe, Ca/Pb, Ca/Ti and Ca/Zn during 2019 that were absent in 2020 suggest that traffic as well as concrete in road dust resuspensions are possible sources.

The strontium content in *T. cordata* leaves from PA during 2019 was more than five times the levels in reference plants established by Pais and Jones (2000), and almost three times the levels observed during 2020 (Table 1; Fig. 2). High Sr contents have been reported recently in other cities in northern Spain, suggesting an edaphic origin of the contamination (Soba et al., 2021). In our case, the same seems to be true due to the high correlation between Sr with Ca and S observed during 2019 (Table 4). A high correlation between Sr and Ca has been observed previously in *Tilia* leaves (Doganlar et al., 2012; Soba et al., 2021), and a significant correlation between absorption of Sr and S has also been identified in plants (Yan et al., 2020), the authors suggested that plant absorb more S to reduce Sr toxicity and migration. Therefore, this is indicating edaphic Sr contamination in PA rather than air pollution, especially during 2019.

In summary, the present work takes advantage of the opportunity offered by the unprecedented COVID-19 lockdown. This has allowed us to study urban air pollution in the same locations for two years with traffic density as a variable factor. As a result, reduction in air pollutants (NO_x, CO and PM_{10}) together with heavy metal in urban tree leaves (Al, Ca, Cu, Fe, Mn, Zn) were measured during COVID-19 lockdown in comparison with the same period in the previous year. After statistical analysis of climatic parameters, traffic density, years, lockdown severity and different pollutants and metals measured by monitoring stations and in tree leaves, we conclude that the main cause for the improvement in urban air pollutants and metals was a reduction in the use of the cars in response to the containment measures to control the disease outbreak. The selected urban locations, although similar in size, present some climatic, economic, and traffic differences that reinforce the main conclusions and make this work relevant for future use by other scientists and law-makers to implement urban mobility measures better adapted to changing times.

4. Conclusions

Lockdown measures due to the outbreak of COVID-19 offered a unique opportunity to identify the source and quantify reductions in urban pollutants. Air pollution data from ground-based urban monitoring stations showed a general decrease in urban air pollutants (NO_x, CO and PM_{10}) in two cities of northern Spain during the spring-summer of 2020 compared with the same period in the previous year. Traffic flow data and the lack of correlations with meteorological data indicate that pollution decreases may not be attributed to meteorological conditions, but to the drastic decline in urban traffic flow due to the COVID-19 lockdown. This result was confirmed through traffic-related metal accumulation in *T. cordata* leaves. In both studied cities, a general decrease in non-pipeline heavy metals (Zn, Fe and Cu) together with a significant decrease in crustal metals related to dust resuspension (Al, Fe, Ti, Mn and Ca) were observed, showing the feasibility of this biomonitoring system as a tool in assessing urban metal pollution. We offer some evidence indicating that the decline in traffic flow substantially decreased NO_x, CO and metals linked to urban pollution, but might cause an increase in other air pollutants such as ozone, which needs to be addressed. The current work presents some direct information to quantify the reduction in pollution due to vehicle restrictions in cities, which in combination with earlier studies may help guide the adoption of regulatory measures to improve air quality and public health on the basis of objective criteria.

Funding

This research was funded by the UPV/EHU-GV IT-1018–16 program (Basque Government).

CRediT authorship contribution statement

David Soba: Experiment design, Sampling, Sample processing, Data curation, Writing original draft and editing. **Angie L. Gámez**: Sampling, Sample processing, Manuscript editing. **José María Becerril:** Experiment design, Sampling, Conceptualization, Writing – review & editing. **Raquel Esteban:** Experiment design, Sampling, Manuscript editing. **Iker Aranjuelo:** Experimental design, Sampling, Writing – review & editing.

Declaration of Competing Interest

The authors declare that they have no known competing financial interests or personal relationships that could have appeared to influence the work reported in this paper.

Acknowledgments

The authors would also like to thank Mr. M. M. Aranjuelo for support given during sample collection. We would also like to thank the City Councils of Pamplona and San Sebastián for providing traffic density data. Finally, the authors also acknowledge support of the publication fee by the CSIC Open Access Publication Support Initiative through its Unit of Information Resources for Research (URICI).

Appendix A. Supporting information

Supplementary data associated with this article can be found in the online version at doi:10.1016/j.ufug.2022.127542.

References

Adachi, K., Tainosho, Y., 2004. Characterization of heavy metal particles embedded in tire dust. Environ. Int. 30, 1009–1017. https://doi.org/10.1016/j.envint.2004.04.004.

Adamiec, E., Jarosz-Krzemińska, E., Wieszała, R., 2016. Heavy metals from non-exhaust vehicle emissions in urban and motorway road dusts. Environ. Monit. Assess. 188, 369. https://doi.org/10.1007/s10661-016-5377-1.

Altuwayjiri, A., Soleimanian, E., Moroni, S., Palomba, P., Borgini, A., De Marco, C., et al., 2021. The impact of stay-home policies during Coronavirus-19 pandemic on the chemical and toxicological characteristics of ambient $PM_{2.5}$ in the metropolitan area of Milan, Italy. Sci. Total Environ. 758. https://doi.org/10.1016/j.scitotenv.2020.143582.

Ambade, B., Sankar, T.K., Kumar, A., Gautam, A.S., Gautam, S., 2021. COVID-19 lockdowns reduce the Black carbon and polycyclic aromatic hydrocarbons of the Asian atmosphere: source apportionment and health hazard evaluation. Environ. Dev. Sustain 3, 1–20. https://doi.org/10.1007/s10668-020-01167-1.

Aničić, M., Spasić, T., Tomašević, M., Rajšić, S., Tasić, M., 2011. Trace elements accumulation and temporal trends in leaves of urban deciduous trees (*Aesculus hippocastanum* and *Tilia* spp.). Ecol. Indic. 11, 824–830. https://doi.org/10.1016/J.ECOLIND.2010.10.009.

Baldasano, J.M., 2020. COVID-19 lockdown effects on air quality by NO2 in the cities of Barcelona and Madrid (Spain). Sci. Total Environ. 741, 140353 https://doi.org/10.1016/j.scitotenv.2020.140353.

Bherwani, H., Nair, M., Musugu, K., Gautam, S., Gupta, A., Kapley, A., Kumar, K., 2020. Valuation of air pollution externalities: comparative assessment of economic damage and emission reduction under COVID-19 lockdown. Air Qual Atmos Health 13, 683–694. https://doi.org/10.1007/s11869-020-00845-3.

Bretzel, F., Calderisi, M., 2006. Metal contamination in urban soils of coastal Tuscany (Italy). Environ. Monit. Assess. 118, 319–335. https://doi.org/10.1007/s10661-006-1495-5.

Briz-Redón, Á., Belenguer-Sapiña, C., Serrano-Aroca, Á., 2021. Changes in air pollution during COVID-19 lockdown in Spain: A multi-city study (/). J. Environ. Sci. 101, 16–26. https://doi.org/10.1016/j.jes.2020.07.029.

Cadle, S.H., Mulawa, P.A., Ball, J., Donase, C., Weibel, A., Sagebie, J.C., Knapp, K.T., Snow, R., 1997. Particulate emission rates from in use high emitting vehicles recruited in Orange County, California. Environ. Sci. Technol. 31, 3405–3412. https://doi.org/10.1021/es9700257.

Choi, Y., Kim, J., Eldering, A., Osterman, G., Yung, Y.L., Gu, Y., Liou, K.N., 2009. Lightning and anthropogenic NOx sources over the United States and the western North Atlantic Ocean: Impact on OLR and radiative effects. Geophys. Res. Lett 36. https://doi.org/10.1029/2009GL039381.

Doganlar, Z.B., Doganlar, O., Erdogan, S., Onal, Y., 2012. Heavy metal pollution and physiological changes in the leaves of some shrub, palm and tree species in urban areas of Adana, Turkey. Chem. Speciat. Bioavailab 24, 65–78. https://doi.org/10.3184/095422912X13338055043100.

Doherty, R.M., Heal, M.R., O'Connor, F.M., 2017. Climate change impacts on human health over Europe through its effect on air quality. Environ Health 16, 118. https://doi.org/10.1186/s12940-017-0325-2.

El-Khatib, A.A., Barakat, N.A., Youssef, N.A., Samir, N.A., 2020. Bioaccumulation of heavy metals air pollutants by urban trees. Int. J. Phytoremediation 22, 210–222. https://doi.org/10.1080/15226514.2019.1652883.

Fan, L., Fu, S., Wang, X., Fu, Q., Jia, H., Xu, H., et al., 2021. Spatiotemporal variations of ambient air pollutants and meteorological influences over typical urban agglomerations in China during the COVID-19 lockdown. J. Environ. Sci. 106, 26–38. https://doi.org/10.1016/j.jes.2021.01.006.

Gautam, S., 2020. COVID-19: air pollution remains low as people stay at home. Air Qual. Atmos. Heal. 13, 853–857. https://doi.org/10.1007/s11869-020-00842-6.

Ghahremanloo, M., Lops, Y., Choi, Y., Yeganeh, B., 2021. Deep learning estimation of daily ground-level NO_2 concentrations from remote sensing data. JGR Atmospheres 126. https://doi.org/10.1029/2021JD034925 e2021JD034925.

Grigoratos, T., Martini, G., 2015. Brake wear particle emissions: a review. Environ. Sci. Pollut. Res. 22, 2491–2504. https://doi.org/10.1007/s11356-014-3696-8.

Grigoratos, T., Samara, C., Voutsa, D., Manoli, E., Kouras, A., 2014. Chemical composition and mass closure of ambient coarse particles at traffic and urban-background sites in Thessaloniki, Greece. Environ. Sci. Pollut. Res. 21, 7708–7722. https://doi.org/10.1007/s11356-014-2732-z.

Guan, W., Ni, Z., Hu, Yu, Liang, W., Ou, C., He, J., Liu, L., et al., 2020. Clinical Characteristics of Coronavirus Disease 2019 in China. N. Engl. J. Med. 382, 1708–1720. https://doi.org/10.1056/NEJMoa2002032.

Guirao, A., 2020. The Covid-19 outbreak in Spain. A simple dynamics model, some lessons, and a theoretical framework for control response. Infect. Dis. Model. 5, 652–669. https://doi.org/10.1016/j.idm.2020.08.010.

Habibi, H., Awal, R., Fares, A., Ghahremanneiad, M., 2020. COVID-19 and the Improvement of the Global Air Quality: The Bright Side of a Pandemic. Atmosphere 11, 1279. https://doi.org/10.3390/atmos11121279.

Han, E., Tan, M.M.J., Turk, E., Sridhar, D., Leung, G.M., Shibuya, K., Asgari, N., Oh, J., García-Basteiro, A.L., Hanefeld, J., Cook, A.R., Hsu, L.Y., Teo, Y.Y., Heymann, D., Clark, H., McKee, M., Legido-Quigley, H., 2020. Lessons learnt from easing COVID-19 restrictions: an analysis of countries and regions in Asia Pacific and Europe. Lancet 396, 1525–1534. https://doi.org/10.1016/S0140-6736(20)32007-9.

Hjortenkrans, D.S.T., Bergbäck, B.G., Häggerud, A.V., 2007. Metal emissions from brake linings and tires: Case studies of Stockholm, Sweden 1995/1998 and 2005. Environ. Sci. Technol. 41, 5224–5230. https://doi.org/10.1021/es070198o.

Huang, D., Li, Q., Wang, X., Li, G., Sun, L., He, B., et al., 2018. Characteristics and Trends of Ambient Ozone and Nitrogen Oxides at Urban, Suburban, and Rural Sites from 2011 to 2017 in Shenzhen, China. Sustainability 10, 4530. https://doi.org/10.3390/su10124530.

Hu, X., Zhang, Y., Ding, Z., Wang, T., Lian, H., Sun, Y., Wu, J., 2012. Bioaccessibility and health risk of arsenic and heavy metals (Cd, Co, Cr, Cu, Ni, Pb, Zn and Mn) in TSP and $PM_{2.5}$ in Nanjing, China. Atmos. Environ. 57, 146–152. https://doi.org/10.1016/j.atmosenv.2012.04.056.

Instituto Nacional de Estadística . (National Statistics Institute), 2019. Cifras oficiales de población resultantes de la revisión del Padrón municipal a 1 de enero [WWW Document]. URL ⟨https://www.ine.es/dynt3/inebase/es/index.htm?padre=517&capsel=522⟩ (accessed 10.10.20).

Jiang, Y., Fan, M., Hu, R., Zhao, J., Wu, Y., 2018. Mosses Are Better than Leaves of Vascular Plants in Monitoring Atmospheric Heavy Metal Pollution in Urban Areas. Int J Environ Res Public Health 15 (6), 1105. https://doi.org/10.3390/ijerph15061105.

Johansson, C., Norman, M., Burman, L., 2009. Road traffic emission factors for heavy metals. Atmos. Environ 43, 4681–4688. https://doi.org/10.1016/j.atmosenv.2008.10.024.

Kalinovic, T.S., Serbula, S.M., Kalinovic, J.V., Radojevic, A.A., Petrovic, J.V., Steharnik, M.M., Milosavljevic, J.S., 2017. Suitability of linden and elder in the assessment of environmental pollution of Brestovac spa and Bor lake (Serbia). Environ. Earth Sci 76, 178. https://doi.org/10.1007/s12665-017-6485-0.

Kukutschová, J., Moravec, P., Tomášek, V., Matějka, V., Smolík, J., Schwarz, J., Seidlerová, J., Šafářová, K., Filip, P., 2011. On airborne nano/micro-sized wear particles released from low-metallic automotive brakes. Environ. Pollut. 159, 998–1006. https://doi.org/10.1016/j.envpol.2010.11.036.

Kumari, P., Toshniwal, D., 2020. Impact of lockdown on air quality over major cities across the globe during COVID-19 pandemic. Urban Clim. 34, 100719 https://doi.org/10.1016/j.uclim.2020.100719.

Li, Yixi, Wang, Y., Rui, X., Li, Yaxiu, Li, Yang, Wang, H., Zuo, J., Tong, Y., 2017. Sources of atmospheric pollution: a bibliometric analysis. Scientometrics 112, 1025–1045. https://doi.org/10.1007/s11192-017-2421-z.

Lough, G.C., Schauer, J.J., Park, J.-S., Shafer, M.M., DeMinter, J.T., Weinstein, J.P., 2005. Emissions of Metals Associated with Motor Vehicle Roadways. Environ. Sci. Technol. 39, 826–836. https://doi.org/10.1021/es048715f.

Marquès, M., Rovira, J., Nadal, M., Domingo, J.L., 2021. Effects of air pollution on the potential transmission and mortality of COVID-19: A preliminary case-study in Tarragona Province (Catalonia, Spain). Environmental Research 192, 110315. https://doi.org/10.1016/j.envres.2020.110315.

Martín, A., Caldelas, C., Weiss, D., Aranjuelo, I., Navarro, E., 2018. Assessment of metal immission in urban environments using elemental concentrations and zinc isotope signatures in leaves of *Nerium oleander*. Environ. Sci. Technol. 52, 2071–2080.

Martorell-Marugán, J., Villatoro-García, J.A., García-Moreno, A., López-Domínguez, R., Requena, F., Merelo, J.J., Lacasaña, M., de Dios Luna, J., Díaz-Mochón, J.J, Lorente, J.A., Carmona-Sáez, P., 2021. DatAC: A visual analytics platform to explore climate and air quality indicators associated with the COVID-19 pandemic in Spain. Sci. Total Environ. 750, 141424. https://doi.org/10.1016/j.scitotenv.2020.141424.

Men, C., Liu, R., Xu, F., Wang, Q., Guo, L., Shen, Z., 2018. Pollution characteristics, risk assessment, and source apportionment of heavy metals in road dust in Beijing, China. Sci. Total Environ. 612, 138–147. https://doi.org/10.1016/j.scitotenv.2017.08.123.

Muhammad, S., Long, X., Salman, M., 2020. COVID-19 pandemic and environmental pollution: A blessing in disguise? Sci. Total Environ. 728, 138820 https://doi.org/10.1016/j.scitotenv.2020.138820.

NCE, National Centre of Epidemiology, Carlos III Health Institute, M. of S. and I., 2020. COVID-19 in Spain [WWW Document]. URL ⟨https://cnecovid.isciii.es/⟩ (accessed 11.18.20).

Pais, I., Jones, J.B., 2000. The Handbook of Trace Elements. St. Lucie Press, Boca Raton, Florida.

Papandreou, C., Arija, V., Aretouli, E., Tsilidis, K.K., Bulló, M., 2020. Comparing eating behaviours, and symptoms of depression and anxiety between Spain and Greece during the COVID-19 outbreak: Cross-sectional analysis of two different confinement strategies. Eur Eat Disorders Rev 28, 836–846. https://doi.org/10.1002/erv.2772.

Piczak, K., Leśniewicz, A., Zyrnicki, W., 2003. Metal concentrations in deciduous tree leaves from urban areas in Poland. Environ. Monit. Assess 86, 273–287. https://doi.org/10.1023/A:1024076504099.

Radzka, E., 2020. The Effect of Meteorological Conditions on Air Pollution in Siedlce. J. Ecol. Eng 21 (1), 97–104. https://doi.org/10.12911/22998993/113074.

Rai, P.K., 2016. Impacts of particulate matter pollution on plants: Implications for environmental biomonitoring. Ecotoxicol. Environ. Saf. 129, 120–136. https://doi.org/10.1016/j.ecoenv.2016.03.012.

Redondo-Bravo, M.J.S., Moros, E.V.M., Sanchez, N., Lorusso, A.C., Ubago, V.G., Garcia, et al., 2020. The first wave of the COVID-19 pandemic in Spain: characterisation of cases and risk factors for severe outcomes, as at 27 April 2020. Euro Surveill 25, 2001431. https://doi.org/10.2807/1560-7917.ES.2020.25.50.2001431.

Sawidis, T., Breuste, J., Mitrovic, M., Pavlovic, P., Tsigaridas, K., 2011. Trees as bioindicator of heavy metal pollution in three European cities. Environ. Poll. 159 (12), 3560–3570. https://doi.org/10.1016/j.envpol.2011.08.008.

Schauer, J.J., Lough, G.C., Shafer, M.M., Christensen, W.F., Arndt, M.F., DeMinter, J.T., Park, J.S., 2006. Characterization of metals emitted from motor vehicles. Res. Rep. Health. Eff. Inst. 133, 1–88.

Serbula, S.M., Kalinovic, T.S., Ilic, A.A., Kalinovic, J.V., Steharnik, M.M., 2013. Assessment of airborne heavy metal pollution using *Pinus* spp. and *Tilia* spp. Aerosol Air Qual. Res 13, 563–573. https://doi.org/10.4209/aaqr.2012.06.0153.

Sicard, P., De Marco, A., Agathokleous, E., Feng, Z., Xu, X., Paoletti, E., et al., 2020. Amplified ozone pollution in cities during the COVID-19 lockdown. Sci. Total Environ. 735, 139542 https://doi.org/10.1016/j.scitotenv.2020.139542.

Skalny, A.V., Lima, T.R.R., Ke, T., Zhou, J.-C., Bornhorst, J., Alekseenko, S.I., Aaseth, J., Anesti, O., Sarigiannis, D.A., Tsatsakis, A., Aschner, M., Tinkov, A.A., 2020. Toxic metal exposure as a possible risk factor for COVID-19 and other respiratory infectious diseases. Food Chem. Toxicol. 146, 111809 https://doi.org/10.1016/j.fct.2020.111809.

Smodiš, B., Pignata, M.L., Saiki, M., Cortés, E., Bangfa, N., Markert, B., Nyarko, B., Arunachalam, J., Garty, J., Vutchkov, M., Wolterbeek, H.T., Steinnes, E., Freitas, M. C., Lucaciu, A., Frontasyeva, M., 2004. Validation and application of plants as biomonitors of trace element atmospheric pollution - A Co-Ordinated effort in 14 countries. J. Atmos. Chem. https://doi.org/10.1007/s10874-004-1210-2.

Soba, D., Gámez, A.L., Úriz, N., Ruiz de Larrinaga, L., Gonzalez-Murua, C., Becerril, J.M., Esteban, R., Serret, D., Araus, J.L., Aranjuelo, I., 2021. Foliar heavy metals and stable isotope (δ^{13}C, δ^{15}N) profiles as reliable urban pollution biomonitoring tools. Urban For. Urban Green. 57, 126918 https://doi.org/10.1016/j.ufug.2020.126918.

Sternbeck, J., Sjödin, Å., Andréasson, K., 2002. Metal emissions from road traffic and the influence of resuspension—results from two tunnel studies. Atmos. Environ. 36, 4735–4744. https://doi.org/10.1016/S1352-2310(02)00561-7.

Tobías, A., Carnerero, C., Reche, C., Massagué, J., Via, M., Minguillón, M.C., Alastuey, A., Querol, X., 2020. Changes in air quality during the lockdown in Barcelona (Spain) one month into the SARS-CoV-2 epidemic. Sci. Total Environ. 726, 138540 https://doi.org/10.1016/j.scitotenv.2020.138540.

Tomašević, M., Rajšić, S., Dordević, D., Tasić, M., Krstić, J., Novaković, V., 2004. Heavy metals accumulation in tree leaves from urban areas. Environ. Chem. Lett. 2, 151–154. https://doi.org/10.1007/s10311-004-0081-8.

Varotsos, K.V., Giannakopoulos, C., Tombrou, M., 2019. Ozone-temperature relationship during the 2003 and 2014 heatwaves in Europe. Reg Environ Change 19, 1653–1665. https://doi.org/10.1007/s10113-019-01498-4.

Wåhlin, P., Berkowicz, R., Palmgren, F., 2006. Characterisation of traffic-generated particulate matter in Copenhagen. Atmos. Environ. 40, 2151–2159. https://doi.org/10.1016/j.atmosenv.2005.11.049.

Wang, C., Horby, P.W., Hayden, F.G., Gao, G.F., 2020. A novel coronavirus outbreak of global health concern. Lancet (London, England) 395, 470–473. https://doi.org/10.1016/S0140-6736(20)30185-9.

Wang, J.M., Jeong, C.-H., Hilker, N., Healy, R.M., Sofowote, U., Debosz, J., Su, Y., Munoz, A., Evans, G.J., 2021. Quantifying metal emissions from vehicular traffic using real world emission factors. Environ. Pollut. 268, 115805 https://doi.org/10.1016/j.envpol.2020.115805.

World Health Organization, 2020, Coronavirus disease (COVID-2019) situation reports online [WWW Document]. URL ⟨https://www.who.int/emergencies/diseases/novel-coronavirus-2019/⟩situation-reports (2020). (accessed 12.7.20).

World Health Organization, 2016, Ambient Air Pollution: A Global Assessment of Exposure and Burden of Disease. Geneva, Switzerland.

Xu, K., Cui, K., Young, L.-H., Hsieh, Y.-K., Wang, Y.-F., Zhang, J., Wan, S., 2020. Impact of the COVID-19 Event on Air Quality in Central China. Aerosol Air Qual. Res 20, 915–929. https://doi.org/10.4209/aaqr.2020.04.0150.

Yan, D., Ding, K., He, Y., Fan, L., Wang, S., Jiang, X., 2020. Strontium Uptake and Effects in Hydroponically Cultivated Celery. Water, Air, Soil Pollut 231, 279. https://doi.org/10.1007/s11270-020-04659-y.

Yushin, N., Chaligava, O., Zinicovscaia, I., Vergel, K., Grozdov, D., 2020. Mosses as bioindicators of heavy metal air pollution in the lockdown period adopted to cope with the COVID-19 pandemic. Atmosphere (Basel) 11. https://doi.org/10.3390/atmos11111194.

Zoran, M.A., Roxana, S.Savastru, R.S, Dan, M., Savastru, D.M., Marina, N., Tautan, M.N., 2020. Assessing the relationship between ground levels of ozone (O3) and nitrogen dioxide (NO_2) with coronavirus (COVID-19) in Milan, Italy. Sci. Total Environ. 740, 140005 https://doi.org/10.1016/j.scitotenv.2020.140005.